Atmos. Chem. Phys., 3, 303–313, 2003
www.atmos-chem-phys.org/acp/3/303/

Atmospheric Chemistry and Physics

Wavelength dependence of isotope fractionation in N_2O photolysis

J. Kaiser[1, 2, 4], **T. Röckmann**[2], **C. A. M. Brenninkmeijer**[1], **and P. J. Crutzen**[1, 3]

[1]Abteilung Chemie der Atmosphäre, Max-Planck-Institut für Chemie, Mainz, Germany
[2]Bereich Atmosphärenphysik, Max-Planck-Institut für Kernphysik, Heidelberg, Germany
[3]Center for Atmospheric Sciences, Scripps Institution of Oceanography, University of California, San Diego, USA
[4]now at: Department of Geosciences, Princeton University, Princeton, New Jersey, USA

Received: 15 July 2002 – Published in Atmos. Chem. Phys. Discuss.: 28 October 2002
Revised: 4 February 2003 – Accepted: 27 February 2003 – Published: 21 March 2003

Abstract. In previous reports on isotopic fractionation in the ultraviolet photolysis of nitrous oxide (N_2O) only enrichments of heavy isotopes in the remaining N_2O fraction have been found. However, most direct photolysis experiments have been performed at wavelengths far from the absorption maximum at 182 nm. Here we present high-precision measurements of the ^{15}N and ^{18}O fractionation constants (ε) in photolysis at 185 nm. Small, but statistically robust depletions of heavy isotopes for the terminal atoms in the linear N_2O molecule are found. This means that the absorption cross sections $\sigma(^{15}N^{14}N^{16}O)$ and $\sigma(^{14}N_2{}^{18}O)$ are larger than $\sigma(^{14}N_2{}^{16}O)$ at this specific wavelength. In contrast, the central N atom becomes enriched in ^{15}N. The corresponding fractionation constants (± 1 standard deviation) are

$$^{15}\varepsilon_1 = \sigma(^{15}N^{14}N^{16}O)/\sigma(^{14}N_2{}^{16}O) - 1 = (3.7 \pm 0.2)\,‰,$$
$$^{18}\varepsilon = \sigma(^{14}N_2{}^{18}O)/\sigma(^{14}N_2{}^{16}O) - 1 = (4.5 \pm 0.2)\,‰ \text{ and}$$
$$^{15}\varepsilon_2 = \sigma(^{14}N^{15}N^{16}O)/\sigma(^{14}N_2{}^{16}O) - 1 = (-18.6 \pm 0.5)‰.$$

To our knowledge, this is the first documented case of such a heavy isotope depletion in the photolysis of N_2O which supports theoretical models and pioneering vacuum ultraviolet spectroscopic measurements of ^{15}N substituted N_2O species that predict fluctuations of ε around zero in this spectral region (Selwyn and Johnston, 1981). Such a variability in isotopic fractionation could have consequences for atmospheric models of N_2O isotopes since actinic flux varies also strongly over narrow wavelength regions between 175 and 200 nm due to the Schumann-Runge bands of oxygen. However, the spacing between maxima and minima of the fractionation constants and of the actinic flux differ by two orders of magnitude in the wavelength domain. The wavelength dependence of fractionation constants in N_2O photolysis can thus be approximated by a linear fit with negligible consequences on the actual value of the spectrally averaged fractionation constant. In order to establish this linear fit, additional measurements at wavelengths other than 185 nm were made using broadband light sources, namely D_2, Hg/Xe and Sb lamps. The latter lamp was used in conjunction with various interference filters to shift the peak photolysis rate to longer wavelengths. From these experiments and existing data in the literature, a comprehensive picture of the wavelength dependence of N_2O photolysis near room-temperature is created.

Correspondence to: J. Kaiser (kaiser@princeton.edu)

1 Introduction

N_2O isotope fractionation by photolysis at various wavelengths has been the subject of at least eight recent experimental studies (Johnston et al., 1995; Rahn et al., 1998; Röckmann et al., 2000, 2001; Toyoda et al., 2001a; Turatti et al., 2000; Umemoto, 1999; Zhang et al., 2000). In line with theoretical calculations (Johnson et al., 2001; Yung and Miller, 1997), the measured fractionation constants exhibit a dependence on the wavelength of photolysis radiation. Photolysis (reaction 1) comprises approximately 90% of the global N_2O sink and is the dominant cause of the observed isotopic enrichment of N_2O in the stratosphere (Griffith et al., 2000; Kim and Craig, 1993; Moore, 1974; Rahn and Wahlen, 1997; Röckmann et al., 2001; Toyoda et al., 2001b; Yoshida and Toyoda, 2000) The remaining 10% of the total N_2O sink are due to the reaction of N_2O with $O(^1D)$ (reactions 2 and 3).

$$N_2O + h\nu \rightarrow N_2 + O(^1D) \quad (185\,\text{nm} < \lambda < 230\,\text{nm}) \quad (90\%) \quad (1)$$
$$N_2O + O(^1D) \rightarrow 2\ NO \quad (6\%) \quad (2)$$
$$N_2O + O(^1D) \rightarrow N_2 + O_2 \quad (4\%) \quad (3)$$

Maximum photolysis rates of N_2O in the stratosphere occur between 195 and 205 nm (Minschwaner et al., 1993), but depending on altitude and latitude there are contributions down to 185 nm and up to 230 nm. Below 185 nm absorption

by O_2 prohibits the penetration of solar light, above 230 nm the photolysis rates are constrained by O_3 absorption and the decrease of the N_2O cross section.

By way of reaction 2, N_2O is the major source of stratospheric NO_x and is thus linked to the O_3 cycle. The tropospheric mixing ratio of N_2O has increased by about 17% from its pre-industrial value and grows by 0.2 to 0.3% per year at present. This must be of concern considering the long atmospheric lifetime of about 120 years (Prather et al., 2001) and the role of N_2O as a greenhouse gas and its potential for O_3 depletion. Thanks to the reduced emissions of organic halogen compounds as demanded by the 1987 Montreal Protocol and its subsequent adjustments and amendments, stratospheric chlorine levels are expected to decrease in the future (WMO, 1999). However, this will reinforce the role of N_2O as a source gas for ozone depleting NO_x radicals (Randeniya et al., 2002). Therefore quantification of N_2O source and sink fluxes are important pieces in global Earth system models. It is hoped that isotope measurements can be used to improve our knowledge of the atmospheric budget of this species, since current estimates suffer from large uncertainties.

Models of atmospheric chemistry and transport require kinetic data on reaction rate constants (k) and photochemical absorption cross sections (σ) as input values. Slight variations of these quantities may occur as a result of isotopic substitution. These kinetic isotope effects are conveniently expressed relative to the most abundant, light species using fractionation factors (α) or fractionation constants (ε). We adopt here the definition of α found in many geological textbooks and used in most previous papers on N_2O isotopologues, but note that it is inverse to custom in chemical kinetics and an IUPAC recommendation (Müller, 1994):

$$\alpha = \frac{k_{\text{heavy}}}{k_{\text{light}}} = 1 + \varepsilon \tag{4}$$

k_{heavy} and k_{light} denote the reaction rate constants of the isotopically heavy and light species (e.g. $^{15}N^{14}N^{16}O$ and $^{14}N_2{}^{16}O$). Photolysis rates (J) are proportional to σ, so that in this case k can be substituted by σ, adopting the recommended value of 1 for the quantum yield of $O(^1D)$ in photolysis of all N_2O isotopologues and isotopomers.

Heavy isotope enrichments in a single sample of stratospheric N_2O were first noticed by Moore (1974), but it took nearly 20 years before the data were backed up by further measurements (Kim and Craig, 1993). Already then, UV photolysis was suspected as origin of the isotopic enrichment. However, a direct measurement at 185 nm found no significant oxygen isotope fractionation at 185 nm (Johnston et al., 1995) and – together with an apparent lack of N_2O sources to balance the atmospheric budget (Watson et al., 1990, 1992) – rekindled speculations about a suite of "non-standard" N_2O sources or sinks (McElroy and Jones, 1996; Prasad, 1997; Wingen and Finlayson-Pitts, 1998; Zipf, 1980). Finally though, a zero point energy (ZPE) model of N_2O photolysis (Yung and Miller, 1997) postulated wavelength-dependent isotopic fractionations: Near-zero fractionations at the absorption maximum of N_2O ($\approx$ 182 nm) were expected as against to isotope enrichments of the residual N_2O at longer and depletions at shorter wavelengths. This explained the stratospheric enrichments (at least qualitatively) and the measurements at 185 nm. In retrospect, this was also in agreement with pioneering vacuum ultraviolet (VUV) spectroscopy of ^{15}N substituted N_2O species (Selwyn and Johnston, 1981), although they seem to have been overlooked at that time. The further prediction of position-dependent enrichments of ^{15}N in the N_2O molecule led to the development of new spectrometric techniques (Brenninkmeijer and Röckmann, 1999; Toyoda and Yoshida, 1999; Turatti et al., 2000). Subsequent tests of this theory found it to be in qualitative agreement with new experimental data, but the measured enrichment constants were always higher than predicted (Rahn et al., 1998; Röckmann et al., 2000, 2001; Toyoda et al., 2001a; Turatti et al., 2000; Umemoto, 1999; Zhang et al., 2000). *Ab initio* calculations by Johnson et al. (2001) gave better fits to the measurements, except for the $^{15}N^{14}N^{16}O$ isotopomer.

Here, we present high-precision measurements of the ^{18}O and of the position-dependent ^{15}N fractionation in room-temperature N_2O photolysis at 185 nm. They validate the existing VUV spectroscopic measurements (Selwyn and Johnston, 1981) and are supplemented by additional measurements with broadband UV light sources. Together with the data from previous reports, a synopsis of the wavelength-dependent isotope fractionation in N_2O photolysis is created which is then used to evaluate the effects of N_2O photolysis in the region of the Schumann-Runge bands on the overall isotopic fractionation.

2 Experimental methods

The change of isotopic composition by photolysis in a closed-system can be described as a Rayleigh fractionation process (Rayleigh, 1896):

$$\delta = y^{\varepsilon} - 1 \tag{5}$$

For applications to isotopes, the so-called δ value is defined here as relative enrichment of the isotope ratio at any time of the reaction (R) against the isotope ratio at the beginning of the reaction: $\delta = R/R_0 - 1$. $y = c/c_0$ is the total remaining fraction of the light isotopologue, but can be equated to a very good degree of approximation with the total remaining N_2O fraction for samples at natural abundance (Kaiser et al., 2002a).

In this study, the calculation of fractionation constants ε was based on a linearised form of Eq. (5) using either the ratio of $\ln(1+\delta)/\ln y$ in each individual experiment or least squares fits to Rayleigh plots of $\ln(1+\delta)$ vs $\ln y$. Given sufficient experimental precision and provided the y-axis offset

in a Rayleigh plot is zero, the latter approach is more suitable to detect influences of reaction parameters on ε.

N_2O in N_2 bath gas was irradiated by different light sources using four reactor types. All gases used were of 99.9999% chemical purity. Reactors A, B and C consist of quartz, stainless steel and borosilicate glass tubes, respectively, and were already used in previous photolysis experiments (Kaiser et al., 2002b; Röckmann et al., 2000). No significant influence of reactor type on the experimental results was found. Reactor E is a borosilicate glass bulb ($V \approx 2.2\,\mathrm{dm}^3$) with a quartz insert (Kaiser et al., 2002a).

The photolysis experiments at 185 nm were performed in reactor E. A pencil style, low-pressure Hg(Ar) lamp ("Pen Ray lamp", LOT Oriel) was put in the quartz insert and usually operated at 18 mA (AC). The spectral output of Pen Ray lamps is known to be remarkably stable and temperature-insensitive, and even the total irradiance is reproducible to within 15% (Reader et al., 1996). The wavelengths of 19 spectral lines in the range 253 to 579 nm were within ± 0.002 nm of published values for Hg emission lines (Sansonetti et al., 1996). However, the 185 nm-line was not investigated. Its intensity relative to the 253.65 nm-line is stated as 3% (LOT Oriel), but may vary from lamp to lamp. Therefore, additional experiments were performed with a second lamp. The precise wavelength of the "185 nm"-line for the natural Hg isotope mixture is given as 184 950 nm (Lide, 1999). Other intense Hg lines in the emission spectrum of these lamps are located at wavelengths > 250 nm and are not of importance for N_2O photolysis.

The irradiation by the lamp led to temperatures of about 50°C at the inner wall of the quartz inset and as high as 100°C at the lamp itself. Therefore, one experiment was conducted at a reduced current of 10 mA, giving only ≈ 40°C and ≈ 85°C, respectively. The temperature of the gas mixture itself was measured with a thermocouple at different positions of the reactor and amounted to fairly homogeneous values of 28°C/25.5°C for 18/10 mA. To check for any influence of O_2 photolysis and subsequent O_3 production on the irradiation spectrum, the quartz cavity was flushed with N_2 during three experiments. The photolysis times varied from 2.1 to 40.9 h, resulting in final yields of 3.5 to 84.5%.

A mixture of 1.0 mmol/mol N_2O/N_2 was used for the experiments at initial pressures of about 1000 mbar. Higher mixing ratios can lead to artefacts which were traced back in a recent study to $O(^1D)$ production by NO_2 photolysis and subsequent reaction of N_2O with $O(^1D)$ (Kaiser et al., 2002b). Pressures were corrected for non-linearity of the sensor and temperature variations. The remaining N_2O fraction (y) was determined by quantitative extraction in an ultra-high efficient Russian Doll-type trap (Brenninkmeijer and Röckmann, 1996). Blank experiments without photolysis gave an indication of the precision of the degree of conversion ($\sigma_{\ln y} = 0.009$) and of the δ values ($\sigma_{\delta^{15}\mathrm{N}} = 0.1$‰; $\sigma_{1\delta^{15}\mathrm{N}} = \sigma_{2\delta^{15}\mathrm{N}} = 0.25$‰; $\sigma_{\delta^{18}\mathrm{O}} = 0.15$‰) from which the fractionation constants are calculated. N_2O samples were purified on a preparatory gas chromatograph (Kaiser et al., manuscript in preparation) and analysed on a Finnigan MAT 252 isotope ratio mass spectrometer for $^{45}\delta$, $^{46}\delta$ and $^{31}\delta$ (Kaiser et al., 2002a). The available Faraday cup configuration of this instrument did not allow to project m/z 30 and m/z 31 beams simultaneously on the centre of a cup. Instead, the cup configuration for O_2 isotope analysis was used and ion currents of the NO^+ fragment were measured on the peak flanks. Thus, precision of the NO^+ fragment analysis was slightly impaired, but by no means compromises the conclusions drawn here.

Photolysis experiments with broadband light sources (D_2, Hg/Xe and Sb lamps, partly used in conjunction with interference filters) were performed with a 4.0 mmol/mol N_2O/N_2 mixture using reactors A to C. The possible presence of an artefact from the reaction of N_2O with $O(^1D)$ for this higher mixing ratio is discussed in Sect. 4. Due to the strong infrared radiation from the Hg/Xe lamp, it was used together with a water filter which protected the photolysis reactor from excessive heating. The filter was filled with high-purity water (MilliQ) and was cooled continuously by water. Unlike the measurements at 185 nm, the $^{31}\delta$ values for the NO^+ fragment were measured on a Micromass Prism II mass-spectrometer with adjustable cups, so that the standard-deviation of $^{31}\delta$ (0.04‰) is comparable to that of $^{45}\delta$ and $^{46}\delta$ (0.02‰ and 0.04‰).

3 Isotopic depletions by N_2O photolysis at 185 nm

The results of photolysis at 185 nm are shown in Figs. 1a and b. Up to the largest degrees of conversion, the fractionation constants give a consistent picture of isotopic depletions at the terminal positions of the residual N_2O (δ^{18}O and $^1\delta^{15}$N). There is no clearly discernible influence of lamp specimen, operating current or nitrogen flushing. The absence of any significant variation of ε with $\ln y$ indicates that most probably no other than the desired fractionation process was taking place, as opposed to the artefacts noticed at higher mixing ratios (Kaiser et al., 2002b). The absence of artefacts was also confirmed by irradiation of an O_2/N_2 mixture (0.62 mmol/mol) for 13.5 h. After the entire extraction and purification procedure, 0.38 μl N_2O (standard ambient temperature and pressure, SATP) were recovered corresponding to the system blank of ≈ 0.3 μl N_2O (SATP). N_2O production from N_2+$O(^1D)$ can thus be neglected, in agreement with its low rate constant of $2.8 \cdot 10^{-36}\ c(\mathrm{N_2})\ \mathrm{cm^6\ s^{-1}}$ (Estupiñán et al., 2002).

Figure 1b shows the directly calculated fractionation constants for each experiment. We argue that the best estimate of the "true" fractionation constants is not the mean of these directly calculated fractionation constants since they are subject to a small error if the y-axis offset in a Rayleigh plot is not exactly zero, especially if the degree of conversion is small ($\ln y \approx 0$). Rather, the slope in a Rayleigh plot

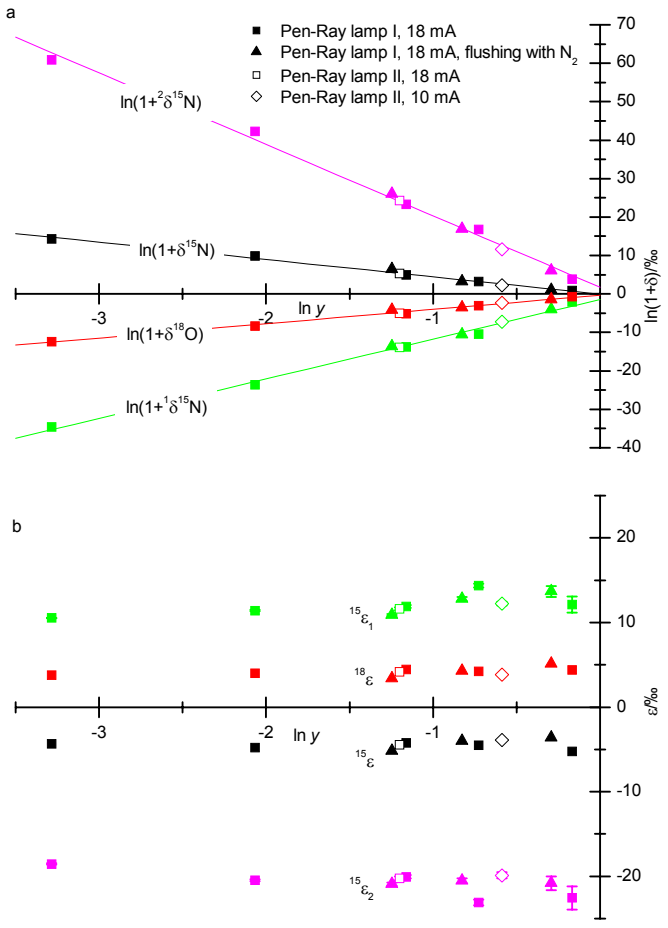

Fig. 1. Rayleigh fractionation plot (panel **a**) of $\ln(1+\delta)$ vs $\ln y$ and directly calculated fractionation constants ε (panel **b**) for photolysis with low-pressure Hg(Ar) lamps at 185 nm. y is the remaining N_2O fraction. Fractionation constants for the terminal and central nitrogen positions in the N_2O molecule are designated $^{15}\varepsilon_1$ and $^{15}\varepsilon_2$; the ^{18}O fractionation is represented by $^{18}\varepsilon$ and the average ^{15}N fractionation by $^{15}\varepsilon = (^{15}\varepsilon_1 + ^{15}\varepsilon_2)/2$. The corresponding δ values are $^1\delta^{15}N$, $^2\delta^{15}N$, $\delta^{18}O$ and $\delta^{15}N$. Two different lamps were used at operating currents of 10 and 18 mA, with or without nitrogen flushing. Errors from N_2O extraction and isotope analysis are smaller than the symbol size, unless indicated.

Table 1. Fractionation constants for N_2O photolysis at 185 nm obtained by different ways of calculation as described in the main text. Errors represent one standard deviation. The y-axis offset of zero for the "mean direct" values corresponds to the calculation of ε from $\ln(1+\delta)/\ln y$

	"mean direct"		"Rayleigh plot"		
	ε/‰	y-axis offset	ε/‰	y-axis offset	r^2
$^{15}\varepsilon$	−4.4±0.5	0	−4.5±0.2	0.0±0.2	0.989
$^{15}\varepsilon_1$	12.2±1.2	0	10.3±0.3	−1.5±0.5	0.992
$^{15}\varepsilon_2$	−20.7±1.3	0	−18.6±0.5	1.7±0.7	0.994
$^{18}\varepsilon$	4.2±0.5	0	3.7±0.1	−0.3±0.2	0.990

(Fig. 1a) is a more reliable estimate of the fractionation constant and is therefore adopted as "true" ε. The results of two calculation methods ("mean direct" and "Rayleigh plot") are shown in Table 1, together with errors at the 1σ level. The positive values for $^{15}\varepsilon_1$ and $^{18}\varepsilon$ are the first documented cases of isotopic depletion in the residual gas by N_2O photolysis.

In contrast to the results presented here, Johnston et al. (1995) did not find any significant oxygen isotope fractionation at 185 nm. Re-analysis of their original data gives $^{18}\varepsilon = (0.2\pm0.2)$‰. Although Johnston and co-workers used a low-pressure mercury resonance lamp powered by a microwave instead of an electrical discharge, differences between the light sources are very unlikely to account for the differences in $^{18}\varepsilon$. In principle, contributions from Hg lines at other wavelengths could have caused the discrepancy in $^{18}\varepsilon$ values, but were not observed for the Pen Ray lamps at wavelengths relevant to N_2O photolysis (i.e. $\lambda < 240$ nm) and were also absent in the spectrum of the microwave powered lamp (Jeff Johnston, personal communication, 2002). Under exceptional conditions such as dramatically increased nitrogen purge flows and reduced plasma voltages, 194.2 nm-emission from Hg^+ was noticed with intensities of up to 20%

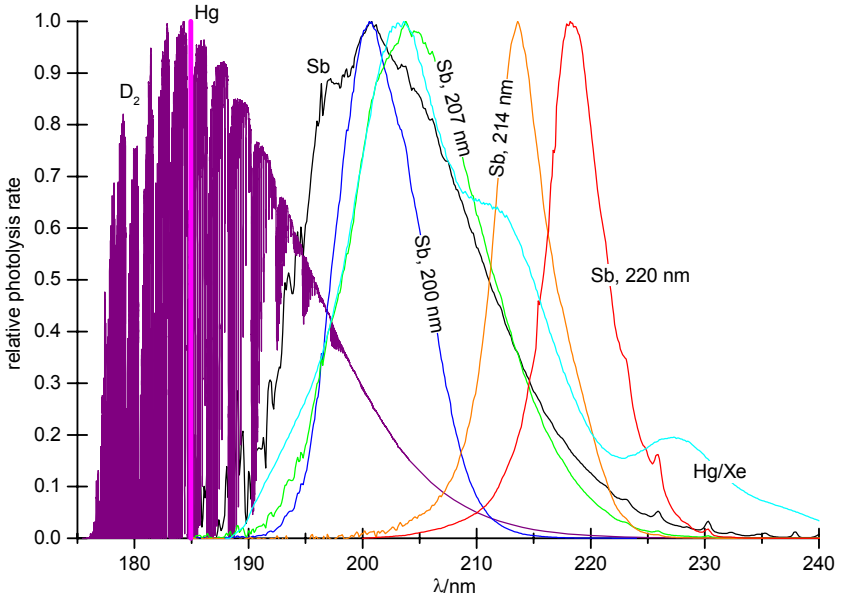

Fig. 2. Relative N_2O photolysis rates for filtered and unfiltered light from different broadband lamps. The photolysis rates have been normalised by division through their maximum values so that they can be compared more easily. The closely spaced O_2 Schumann-Runge bands account for the structured appearance of the D_2 lamp spectrum.

Table 2. Fractionation constants for N_2O photolysis with broadband light sources

ε/‰	D_2 lamp	HgXe lamp	Sb lamp, 200 nm filter	Sb lamp, 214 nm filter	Sb lamp, 220 nm filter
$^{15}\varepsilon$	−20.0±0.1	−48.9±1.5	−39±7	−59±10	−69±5
$^{15}\varepsilon_1$	−8.4±0.4	−28.1±2.1	*n.a.*[a]	−41±7	−43±3
$^{15}\varepsilon_2$	−31.4±0.3	−69.5±2.8	*n.a.*[a]	−74±13	−95±7
$^{18}\varepsilon$	−15.9±0.1	−46.9±1.9	−43±8	−52±9	−61±5
$\ln \hat{y}^b$	−1.2	−0.39	−0.040	−0.034	−0.076

[a] *n.a.*: not analysed
[b] $\hat{y}$: maximum degree of conversion

relative to the 185 nm-line (Cantrell et al., 1997; Lanzendorf et al., 1997), but under thermally normal operating conditions the relative emission intensity does not exceed a few percent. Analytical errors are more probable to be blamed for the discrepancy between the two studies: Rather than analysing N_2O directly, Johnston et al. decomposed it first to N_2 and O_2 in a quartz tube with gold insert at $> 800°C$ and separated N_2 and O_2 afterwards (Cliff and Thiemens, 1994), since they wanted to analyse $^{17}O/^{16}O$ variations as well. If separation of N_2 from O_2 is not quantitative, this may compromise the accuracy of the $\delta^{18}O$ and especially $\delta^{17}O$ values, because N_2 may interfere with O_2 isotope measurements (Sowers et al., 1989). This interference is likely to be mass-spectrometer specific and is presumably caused by stray N_2^+ ions reaching the Faraday cup collectors for O_2 species. The unlikely slope of a $\ln(1+\delta^{17}O)$ vs $\ln(1+\delta^{18}O)$ plot of -1.5 ± 0.4 derived from re-analysis of Johnston et al.'s data set lends support to this interpretation. A more realistic value of this slope should be close to 0.5.

4 Photolysis with broadband light sources

Additional photolysis experiments were performed with a set of different broadband light sources. The corresponding spectral photolysis rates (Fig. 2) were calculated from direct measurements of the emission spectra of the Sb (Röckmann et al., 2001) and Hg/Xe lamps (Saueressig, 1999), convoluted (where appropriate) with transmission spectra of four interference filters (Melles Griot) and the N_2O absorption spectrum at room temperature (Selwyn et al., 1977; Yoshino et al., 1984). The emission spectrum of the D_2 lamp was not measured directly, but was calculated from measurements of the spectral radiant intensity of a D_2 calibration lamp (Mathias Richter, personal communication, 2001), transmission functions of synthetic silica windows (Hamamatsu) and high-resolution O_2 absorption cross sections (Minschwaner et al., 1992).

Photolysis half-life times were about 11 h for the D_2 lamp and 63 h for the Hg/Xe lamp. Thus, sufficient degrees of

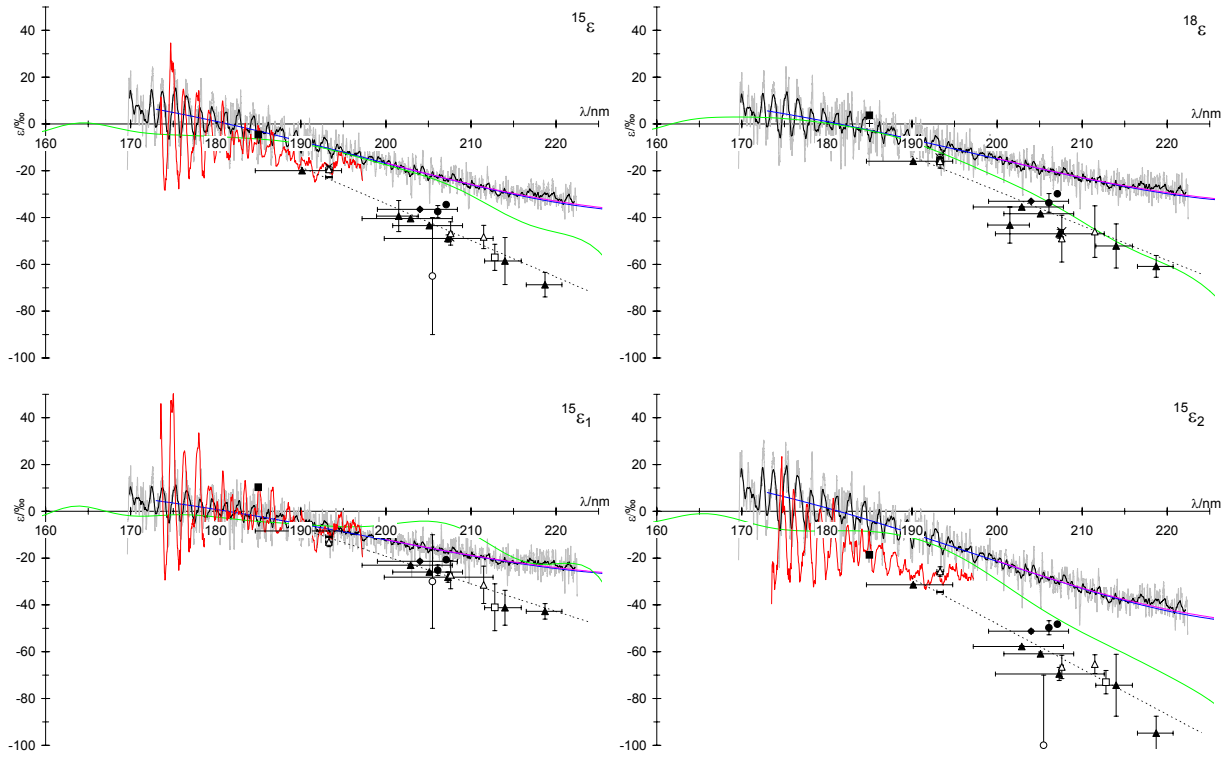

Fig. 3. Measured and theoretically predicted fractionation constants for N_2O photolysis at room temperature (unless indicated)

conversion were achieved within reasonable irradiation time (extending up to 22 and 33 h, respectively), and the fractionation constants derived from Rayleigh plots have small errors (Table 2).

The fractionation constants measured with the unfiltered Sb lamp and in combination with the 207 nm filter (20 nm FWHM) have been presented before (Kaiser et al., 2002b; Röckmann et al., 2001). To confine the spectrum of the Sb lamp to narrower wavelength regions, 200 nm, 214 nm and 220 nm filters were used in spectral bandwidths of 10 nm (FWHM). However, this also reduced the light available for photolysis and considerably lengthened the required irradiation times. This was aggravated by the low peak transmissions of the filters (13 to 18%) and by light loss due to the fact that the extensive discharge of the Sb lamp could not be well focussed on the filter diameter of 25 mm. Therefore, only small extents of photolysis could be achieved within reasonable times, e.g. after 216 h of irradiation with the 220 nm

filter $\ln y$ was only -0.076. Furthermore, the 200 nm filter went blind after 72 h total irradiation time. Rayleigh plots of $\ln(1+\delta)$ are still well approximated by linear fits to $\ln y$, but the error introduced by the extraction procedure is not negligible anymore at these low extents of photolysis. Determined from blank runs, the average standard deviation of $\ln y$ is $\sigma_{\ln y} = 0.004$ for reactors A to C. This is smaller than for reactor E, probably because of the better reproducibility of the manual extraction procedure for smaller reactor sizes. Following Williamson (1968) and York (1966) linear least-squares fits are applied to the data that take into account the mass-spectrometric errors of $\ln(1+\delta)$ and assume an invariable error of 0.004 for $\ln y$. Therefore the calculated fractionation constants for the experiments with Sb lamp and the 200, 214 and 220 nm filters have larger errors (Table 2). The approach by Williamson/York has the advantage over a simple linear least squares fit that it considers errors of both dependent and independent variables and that it is symmetric with respect to co-ordinate exchange.

We note that these broadband photolysis measurements were obtained with an N_2O mixing ratio of 4.0 mmol/mol. This may introduce artefacts by interference of the reaction of N_2O + $O(^1D)$ as discussed for high-precision measurements at 1.0 and 4.0 mmol/mol with the Sb lamp (Kaiser et al., 2002b). The necessary upward corrections depend on $\ln y$, the "true" values for ε and the lamp spectrum. Extrapolating the empirical formula derived for the Sb lamp with and without 207 nm interference filter (Kaiser et al., 2002b) to correct the fractionation constants measured here, gives upward revisions of $\Delta|^{15}\varepsilon_2| = 6‰$ at $\ln y = -0.39$ for the Hg/Xe lamp as the worst case. However, considering the different emission spectra, a direct extrapolation might not be justified. Therefore and since the estimated correction is only $2\sigma_{^{15}\varepsilon_2}$, we leave the measurements uncorrected. It should be noted that corrections could be warranted for the results of other studies, too, but are difficult to quantify in retrospect.

5 Synoptic view of the wavelength dependence

Figure 3 is an overview of measured and theoretically predicted ε values plotted against wavelength, including the data from this paper. In general, both experimental data and theoretical predictions qualitatively agree on increasing enrichments at higher wavelengths and the order $^{15}\varepsilon_2 < ^{18}\varepsilon < ^{15}\varepsilon_1$, but differ in the magnitudes of ε as well as in its sign near the absorption maximum at 182 nm. The experimental results are approximated by a linear fit from 190 to 220 nm (Table 3).

Data were adopted from the original publications and are presented with 1σ y-error bars as stated by the authors. Experimental data from laser photolysis mostly represent "single wavelengths" except for the measurements with ArF lasers at 193.3 nm which were performed at the natural linewidth of 0.7 nm (FWHM). In case of the broadband photolysis experiments, data points are located at the median wavelengths for 50% photolysis. The "x-error bars" indicate the 25% and 75% quartiles. If these quartiles are symmetric about the median and if the slope $\partial\varepsilon/\partial\lambda$ does not change too much over the range of photolysis, the fractionation constant is close to a hypothetical "single wavelength" measurement at the median λ. Since the actual slope $\partial\varepsilon/\partial\lambda$ appears to be almost constant between 190 and 220 nm and the spectral photolysis rates of the broadband light sources are fairly symmetric indeed about their median wavelength (Fig. 2), this explains the relative good agreement between broadband and "single wavelength" data. The weighted linear fit shown in Fig. 3 therefore only considers the errors of ε.

Table 3. Parameters for a y-error weighted linear fit of the wavelength dependence of ε derived from the results of N_2O photolysis experiments (Fig. 3): $\varepsilon = \varepsilon(200\,\text{nm}) + \partial\varepsilon/\partial\lambda(\lambda - 200\,\text{nm})$

	$\partial\varepsilon/\partial\lambda$ (‰/nm)	2σ	$\varepsilon(200\,\text{nm})$ (‰)	2σ
$^{15}\varepsilon$	−1.57	0.03	−34.1	0.2
$^{15}\varepsilon_1$	−1.18	0.04	−19.2	0.2
$^{15}\varepsilon_2$	−1.94	0.05	−48.1	0.4
$^{18}\varepsilon$	−1.48	0.03	−28.6	0.2

The fractionation constants of the ^{15}N isotopomers measured by direct photolysis experiments are complemented by VUV spectroscopic measurements between 173 and 197 nm (Selwyn and Johnston, 1981). The cross-sections are used to calculate ε. The "fine-structure" of ε is in good agreement with the "single wavelength" measurements at 185 and 193.3 nm (Fig. 4) and lends support to the view that the VUV spectroscopic data are most probably adequate to represent the high resolution fractionation constants within their wavelength range. Unfortunately, this range ends at 197 nm, short of the 195–205 nm region most important for stratospheric N_2O photolysis.

The fractionation constants predicted by the zero point energy (ZPE) theory (Miller and Yung, 2000; Yung and Miller, 1997) have been derived by blue-shifting the high resolution absorption spectrum of Yoshino et al. (1984) in addition to the polynomial approximations of $\ln\sigma$ proposed by Selwyn et al. (1977) and Mérienne et al. (1990), assuming that these spectra represent essentially the absorption cross section of the most abundant N_2O species, $^{14}N_2{}^{16}O$. Although the relative order of ^{18}O and position-dependent ^{15}N fractionations is predicted correctly, their magnitudes are about a factor of 2 too low. Also, at wavelengths close to the absorption maximum, the theoretical "fine structure" is not in phase with VUV spectroscopic measurements (Fig. 4).

The *ab initio* calculations by Johnson et al. (2001) were performed using the Hermite propagator (HP) on a two-dimensional (2-D) potential energy surface (PES) (spanned

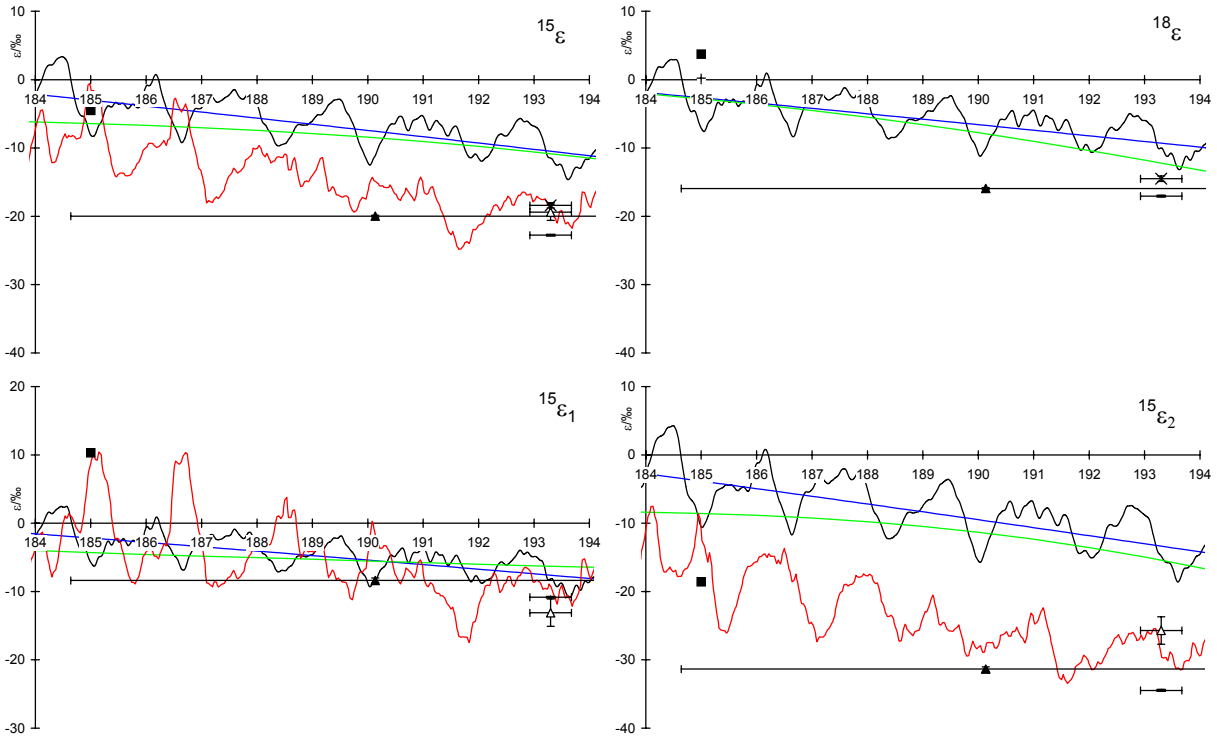

Fig. 4. Comparison between fractionation constants derived from theoretical predictions, direct measurements and VUV spectroscopy in the range from 184 to 194 nm. The same symbols as in Fig. 3 have been used, but the high-resolution ZPE calculation has been omitted for clarity.

by NN-O distance and bending angle) at 1 nm resolution and therefore lack the "fine structure" seen in the ZPE predictions and VUV spectroscopic measurements (Matthew S. Johnson, personal communication, 2002). The agreement with the measurements is good for $^{14}N_2{}^{18}O$ and better than the ZPE theory for $^{14}N^{15}N^{16}O$, but $^{15}N^{14}N^{16}O$ is not adequately modelled, also as a consequence of the 2-D-PES.

6 Implications for the stratosphere and modelling

For stratospheric modelling, one now has the choice between various data sets. Considering the underestimated fractionation constants of the theoretical predictions (except for $^{18}\varepsilon$ in the HP model), it seems that the linear fit through the experimental data represents the wavelength dependence of ε more adequately. This fit also agrees reasonably well with the VUV spectroscopic measurements up to 197 nm. In a separate publication (Kaiser et al., 2002b), we have presented temperature dependent measurements of fractionation constants for broadband photolysis with the Sb lamp (median wavelength: 203 nm). At lower temperatures, the HP theory predictions compared slightly better to the experimental measurements than at room temperature, but were still off by more than a factor of two for $^{15}N^{14}N^{16}O$, underscoring the remaining deficiencies of the model. However, one has to be careful in extrapolating the derived temperature dependence to other wavelengths, e.g. values of $^{15}\varepsilon_2$ derived from the VUV spectroscopic measurements at 197 nm and 213 K were identical to those for broadband photolysis at the same temperature and longer wavelengths. This seems to imply a constant value of $^{15}\varepsilon_2$ between 197 and $\approx$ 203 nm, in disagreement to the observed wavelength-dependence at room temperature. However, errors in the VUV spectroscopic cross-sections could also account for this discrepancy and cannot be entirely excluded.

Using the validated VUV spectroscopic measurements, we can now consider additional complications for atmospheric modelling from the "oscillations" and changes of sign of ε below 190 nm. Due to the strong variation of actinic flux over narrow wavelength regions in the Schumann-Runge bands below 200 nm, this may have noticeable influences on the fractionation constants. We have therefore calculated the expected fractionation constants for photolysis using actinic fluxes at 20, 40 and 80 km (US standard atmosphere, solar zenith angle 30°) (Minschwaner et al., 1993). The data were averaged to about 0.1 nm resolution in the Schumann-Runge region and to about 1 nm above 200 nm. This is more than sufficient to sample the maximum and minimum values of the N_2O fractionation constants which occur with a period of about 2 nm. Altitudes of 20 and 40 km are below and above the region of maximum N_2O photolysis in the at-

Table 4. Calculated fractionation constants for N_2O photolysis at 20, 40 and 80 km (US standard atmosphere, solar zenith angle: 30°)

	Scenario	ε(20 km)	ε(40 km)	ε(80 km)
$^{15}\varepsilon_1$/‰	1	−21.88	−22.56	−16.25
	2	−21.88	−22.53	−16.32
$^{15}\varepsilon_2$/‰	1	−52.57	−53.52	−43.11
	2	−52.57	−53.63	−43.42

mosphere and should therefore provide limits for the fractionation constants. Mesospheric N_2O photolysis at 80 km is negligible, but has been included for comparison. Given the sparse database at lower temperatures, we restrict our calculations to room temperature, although this is clearly not representative for the stratosphere and mesosphere. However, the vibrational structures in the N_2O absorption spectrum become less intense with lower temperatures (Selwyn and Johnston, 1981) and so should the oscillations in ε. Therefore, the room temperature calculations are a "worst-case" scenario for any interference of Schumann-Runge bands and N_2O isotope fractionation. Two scenarios have been investigated: The first one was created from the high-resolution VUV spectroscopic data for $^{15}\varepsilon_2$ and $^{15}\varepsilon_1$ (Selwyn and Johnston, 1981) up to 190 nm, complemented by the linear fit (Fig. 3) for higher wavelengths. In the second scenario, the linear fit is extrapolated also to wavelengths below 190 nm. For the sake of argument, the linear fit is extended in both scenarios to wavelengths up to 240 nm. Any errors thus introduced will be minor due to the small contribution of this wavelength range to the total N_2O loss at all three altitudes. Table 4 shows the results of the calculations.

Interestingly, the differences between scenario 1 and 2 are negligible for both fractionation constants and all altitudes. More surprising is the small altitude dependence of ε. There is barely any variation in ε at 20 km and at 40 km due to the change of actinic flux. The minute increase of $|\varepsilon|$ with altitude is in line with previous qualitative considerations which postulated an increase of $|\varepsilon|$ with altitude due to the decreasing influence of O_3 absorption in the Hartley band (Yoshida and Toyoda, 2000). The negligible difference between scenarios 1 and 2 is a consequence of the different spacing between individual rotational lines in the Schumann-Runge bands ($\approx$ 175 to $\approx$ 200 nm) and the vibrational structure in the N_2O UV absorption spectrum ($\approx$ 170 to $\approx$ 190 nm).

7 Conclusions

The new photolysis measurements at 185 nm have demonstrated for the first-time heavy isotope depletions in the residual gas of N_2O photolysis experiments. The absorption cross-sections of N_2O species with isotopic substitutions at the terminal positions of the molecule are larger than for the most abundant $^{14}N_2{}^{16}O$ isotopologue, corresponding to an inverse kinetic isotope effect. In contrast, isotope enrichments are observed at the central nitrogen position as found at longer wavelengths in other studies.

Taken together with measurements of "single wavelength photolysis" at 193.3 nm and of broadband photolysis by a D_2 lamp with a median wavelength for N_2O photolysis of 190 nm, these results serve to validate existing VUV spectroscopic measurements of ^{15}N isotopomers in the wavelength range from 173 to 197 nm. However, most of the atmospheric N_2O photolysis occurs at wavelengths from 195 to 205 nm, warranting an extension of the high-resolution spectroscopic analyses of isotopically substituted N_2O species to longer wavelengths. This should cover the whole range of stratospherically relevant temperatures (200 to 300 K) and should also include ^{17}O and ^{18}O isotopologues. For the moment, the existing experimental data can be used to create a comprehensive view of the wavelength dependence of isotope fractionation in N_2O photolysis. A linear fit to the data in the range from 190 to 220 nm describes the existing measurements of $^{15}\varepsilon$, $^{15}\varepsilon_1$, $^{15}\varepsilon_2$ and $^{18}\varepsilon$ quite well (Table 3).

An estimation of the dependence of fractionation constants on changes of actinic flux with altitude has shown that the average fractionation constants are only negligibly affected between 20 and 40 km. The contribution of isotopic fractionation by photolysis in the region of O_2 Schumann-Runge bands can be well approximated by an extension of the linear fit derived from the photolysis experiments.

Acknowledgement. Many thanks to Ken Minschwaner for the actinic flux data, to Matt Johnson for the results from the HP theory calculations, to Mathias Richter for the D_2 lamp spectrum, to John Crowley for spectroscopic measurements and to Lukas Baumgartner for access to the Prism II mass spectrometer. This paper also benefited from numerous useful discussions with these colleagues as well as valuable contributions from Christoph Brühl, Terry Dillon, Ralf Dreiskemper, Abraham Horowitz, Jeff Johnston, Hannelore Keller-Rudek, Tae Siek Rhee and Verena Trautner.

References

Brenninkmeijer, C. A. M. and Röckmann, T.: Russian doll type cryogenic traps: Improved design and isotope separation effects, Anal. Chem., 68 (17), 3050–3053, 1996.

Brenninkmeijer, C. A. M. and Röckmann, T.: Mass spectrometry of the intramolecular nitrogen isotope distribution of environmental nitrous oxide using fragment-ion analysis, Rapid Commun. Mass Spectrom., 13 (20), 2028–2033, 1999.

Cantrell, C. A., Zimmer, A., and Tyndall, G. S.: Absorption cross sections for water vapor from 183 to 193 nm, Geophys. Res. Lett., 24 (17), 2195–2198, 1997.

Cliff, S. S. and Thiemens, M. H.: High-precision isotopic determination of the $^{18}O/^{16}O$ and $^{17}O/^{16}O$ ratios in nitrous oxide, Anal. Chem., 66 (17), 2791–2793, 1994.

Estupiñán, E. G., Stickel, R. E., Nicovich, J. M., and Wine, P. H.: Investigation of N_2O production from 266 and 532 nm laser flash

photolysis of $O_3/N_2/O_2$, J. Phys. Chem. A, 106 (24), 5880–5890, 2002.

Griffith, D. W. T., Toon, G. C., Sen, B., Blavier, J.-F., and Toth, R. A.: Vertical profiles of nitrous oxide isotopomer fractionation measured in the stratosphere, Geophys. Res. Lett., 27 (16), 2485–2488, 2000.

Johnson, M. S., Billing, G. D., Gruodis, A., and Janssen, M. H. M.: Photolysis of nitrous oxide isotopomers studied by time-dependent Hermite propagation, J. Phys. Chem. A, 105 (38), 8672–8680, 2001.

Johnston, J. C., Cliff, S. S., and Thiemens, M. H.: Measurement of multioxygen isotopic ($\delta^{18}O$ and $\delta^{17}O$) fractionation factors in the stratospheric sink reactions of nitrous oxide, J. Geophys. Res., 100 (D8), 16 801–16 804, 1995.

Kaiser, J., Brenninkmeijer, C. A. M., and Röckmann, T.: Intramolecular ^{15}N and ^{18}O fractionation in the reaction of N_2O with $O(^1D)$ and its implications for the stratospheric N_2O isotope signature, J. Geophys. Res., 107 (D14), 4214, doi: 10.1029/2001JD001506, 2002a.

Kaiser, J., Röckmann, T., and Brenninkmeijer, C. A. M.: Temperature dependence of isotope fractionation in N_2O photolysis, Phys. Chem. Chem. Phys., 4 (18), 4220–4230, doi: 10.1039/B204837J, 2002b.

Kim, K.-R. and Craig, H.: Nitrogen-15 and oxygen-18 characteristics of nitrous oxide: A global perspective, Science, 262 (5141), 1855–1857, 1993.

Lanzendorf, E. J., Hanisco, T. F., Donahue, N. M., and Wennberg, P. O.: Comment on: "The measurement of tropospheric OH radicals by laser-induced fluorescence spectroscopy during the POPCORN field campaign" by Hofzumahaus et al. and "Intercomparison of tropospheric OH radical measurements by multiple folded long-path laser absorption and laser induced fluorescence" by Brauers et al., Geophys. Res. Lett., 24 (23), 3037–3038, 1997.

Lide, D. R.: CRC Handbook of Chemistry Physics, CRC Press, Boca Raton, 1999.

McElroy, M. B. and Jones, D. B. A.: Evidence for an additional source of atmospheric N_2O, Global Biogeochem. Cycles, 10 (4), 651–659, 1996.

Mérienne, M. F., Coquart, B., and Jenouvrier, A.: Temperature effect on the ultraviolet absorption of $CFCl_3$, CF_2Cl_2, and N_2O, Planet. Space Sci., 38 (5), 617–625, 1990.

Miller, C. E. and Yung, Y. L.: Photo-induced isotopic fractionation of stratospheric N_2O, Chemosphere: Global Change Sci., 2, 255–266, 2000.

Minschwaner, K., Anderson, G. P., Hall, L. A., and Yoshino, K.: Polynomial coefficients for calculating O_2 Schumann-Runge cross sections at 0.5 cm^{-1} resolution, J. Geophys. Res., 97 (D9), 10 103–10 108, 1992.

Minschwaner, K., Salawitch, R. J., and McElroy, M. B.: Absorption of solar radiation by O_2: Implications for O_3 and lifetimes of N_2O, $CFCl_3$, and CF_2Cl_2, J. Geophys. Res., 98 (D6), 10 543–10 561, 1993.

Moore, H.: Isotopic measurement of atmospheric nitrogen compounds, Tellus, 26 (1/2), 169–174, 1974.

Müller, P.: Glossary of terms used in physical organic chemistry, Pure Appl. Chem., 66, 1077–1184, 1994.

Prasad, S. S.: Potential atmospheric sources and sinks of nitrous oxide: 2. Possibilities from excited O_2, "embryonic" O_3, and optically pumped excited O_3, J. Geophys. Res., 102 (D17), 21 527–21 536, 1997.

Prather, M., Ehhalt, D., Dentener, F., Derwent, R., Dlugokencky, E., Holland, E., Isaksen, I., Katima, J., Kirchhoff, V., Matson, P., Midgley, P., and Wang, M.: Atmospheric chemistry and greenhouse gases, in: Climate Change 2001: The Scientific Basis: Contribution of Working Group I to the Third Assessment Report of the Intergovernmental Panel of Climate Change, (Eds) Houghton, J. T., Ding, Y., Griggs, D. J., Noguer, M., van der Linden, P. J., Dai, X., Maskell, K., and Johnson, C.A., pp. 239–287, Cambridge University Press, Cambridge, United Kingdom and New York, NY, USA, 2001.

Rahn, T. and Wahlen, M.: Stable isotope enrichment in stratospheric nitrous oxide, Science, 278 (5344), 1776–1778, 1997.

Rahn, T., Zhang, H., Wahlen, M., and Blake, G. A.: Stable isotope fractionation during ultraviolet photolysis of N_2O, Geophys. Res. Lett., 25 (24), 4489–4492, 1998.

Randeniya, L. K., Vohralik, P. F., and Plumb, I. C.: Stratospheric ozone depletion at northern mid latitudes in the 21st century: The importance of future concentrations of greenhouse gases nitrous oxide and methane, Geophys. Res. Lett., 29 (4), 4, 2002.

Rayleigh, J. W. S.: Theoretical considerations respecting the separation of gases by diffusion and similar processes, Philos. Mag., S. 5, 42, 493–498, 1896.

Reader, J., Sansonetti, C. J., and Bridges, J. M.: Irradiances of spectral lines in mercury pencil lamps, Appl. Opt., 35 (1), 78–83, 1996.

Röckmann, T., Brenninkmeijer, C. A. M., Wollenhaupt, M., Crowley, J. N., and Crutzen, P. J.: Measurement of the isotopic fractionation of $^{15}N^{14}N^{16}O$, $^{14}N^{15}N^{16}O$ and $^{14}N^{14}N^{18}O$ in the UV photolysis of nitrous oxide, Geophys. Res. Lett., 27 (9), 1399–1402, 2000.

Röckmann, T., Kaiser, J., Brenninkmeijer, C. A. M., Crowley, J. N., Borchers, R., Brand, W. A., and Crutzen, P. J.: The isotopic enrichment of nitrous oxide ($^{15}N^{14}NO$, $^{14}N^{15}NO$, $^{14}N^{14}N^{18}O$) in the stratosphere and in the laboratory, J. Geophys. Res., 106 (D10), 10 403–10 410, 2001.

Sansonetti, C. J., Salit, M. L., and Reader, J.: Wavelengths of spectral lines in mercury pencil lamps, Appl. Opt., 35 (1), 74–77, 1996.

Saueressig, G.: Bestimmung von kinetischen Isotopentrennfaktoren in den atmosphärischen Methanabbaureaktionen, Ph. D. thesis, Johannes-Gutenberg-Universität, Mainz, 1999.

Selwyn, G., Podolske, J., and Johnston, H. S.: Nitrous oxide ultraviolet absorption spectrum at stratospheric temperatures, Geophys. Res. Lett., 4 (10), 427–430, 1977.

Selwyn, G. S. and Johnston, H. S.: Ultraviolet absorption spectrum of nitrous oxide as function of temperature and isotopic substitution, J. Chem. Phys., 74 (7), 3791–3803, 1981.

Sowers, T., Bender, M., and Raynaud, D.: Elemental and isotopic composition of occluded O_2 and N_2 in polar ice, J. Geophys. Res., 94 (D4), 5137–5150, 1989.

Toyoda, S. and Yoshida, N.: Determination of nitrogen isotopomers of nitrous oxide on a modified isotope ratio mass spectrometer, Anal. Chem., 71 (20), 4711–4718, 1999.

Toyoda, S., Yoshida, N., Suzuki, T., Tsuji, K., and Shibuya, K.: Isotopomer fractionation during photolysis of nitrous oxide by ultraviolet of 206 to 210 nm, in: International Conference on the Study of Environmental Change Using Isotope Techniques,

edited by IAEA, International Atomic Energy Agency, Vienna, Austria, 2001a.

Toyoda, S., Yoshida, N., Urabe, T., Aoki, S., Nakazawa, T., Sugawara, S., and Honda, H.: Fractionation of N_2O isotopomers in the stratosphere, J. Geophys. Res., 106 (D7), 7515–7522, 2001b.

Turatti, F., Griffith, D. W. T., Wilson, S. R., Esler, M. B., Rahn, T., Zhang, H., and Blake, G. A.: Positionally dependent ^{15}N fractionation factors in the UV photolysis of N_2O determined by high resolution FTIR spectroscopy, Geophys. Res. Lett., 27 (16), 2489–2492, 2000.

Umemoto, H.: $^{14}N/^{15}N$ isotope effect in the UV photodissociation of N_2O, Chem. Phys. Lett., 314, 267–272, 1999.

Watson, R. T., Meira Filho, L. G., Sanhueza, E., and Janetos, A.: Greenhouse gases: Sources and sinks, in: Climate Change: The IPCC Scientific Assessment, (Eds) Houghton, J.T., Callander, B. A., and Varney, S. K., pp. 29–46, Cambridge University Press, Cambridge, UK, 1992.

Watson, R. T., Rodhe, H., Oeschger, H., and Siegenthaler, U.: Greenhouse gases and aerosols, in: Climate Change: The IPCC Scientific Assessment, (Eds) Houghton, J. T., Jenkins, G. J., and Ephraums, J. J., pp. 5–40, Cambridge University Press, New York, 1990.

Williamson, J. H.: Least-squares fitting of a straight line, Can. J. Phys., 46, 1845–1847, 1968.

Wingen, L. M. and Finlayson-Pitts, B. J.: An upper limit on the production of N_2O from the reaction of $O(^1D)$ with CO_2 in the presence of N_2, Geophys. Res. Lett., 25 (4), 517–520, 1998.

WMO: Scientific Assessment of Ozone Depletion: 1998. Global Ozone Research and Monitoring Project, 732 pp., World Meteorological Organization, Geneva, Switzerland, 1999.

York, D.: Least-squares fitting of a straight line, Can. J. Phys., 44 (5), 1079–1086, 1966.

Yoshida, N. and Toyoda, S.: Constraining the atmospheric N_2O budget from intramolecular site preference in N_2O isotopomers, Nature, 405, 330–334, 2000.

Yoshino, K., Freeman, D. E., and Parkinson, W. H.: High resolution absorption cross section measurements of N_2O at 295–299 K in the wavelength region 170–222 nm, Planet. Space Sci., 32 (10), 1219–1222, 1984.

Yung, Y. L. and Miller, C. E.: Isotopic fractionation of stratospheric nitrous oxide, Science, 278 (5344), 1778–1780, 1997.

Zhang, H., Wennberg, P. O., Wu, V. H., and Blake, G. A.: Fractionation of $^{14}N^{15}N^{16}O$ and $^{15}N^{14}N^{16}O$ during photolysis at 213 nm, Geophys. Res. Lett., 27 (16), 2481–2484, 2000.

Zipf, E. C.: A laboratory study on the formation of nitrous oxide by the reaction $N_2(A^3\sum_u^+) + O_2 \rightarrow N_2O + O$, Nature, 287, 523–524, 1980.